Nonlinear Effects at Woodwind Toneholes

N. Giordano
Auburn University, 246 Sciences Center Classroom Building, Auburn, Al, AK 36849, USA
njg0003@auburn.edu

Direct numerical simulations of the aeroacoustics of the recorder are used to study the flow of air near a tonehole. Our calculations are based on the Navier-Stokes equations and are thus able to study the nonlinear effects that occur at high sound pressure levels. We find, in agreement with experimental work, that nonlinear effects are largest on the downstream edge of a tonehole that is inside the recorder tube. Quantitative results for the velocity field are presented and the effect of undercutting the tonehole is also described.

1 Introduction

Physical modeling of musical instruments has advanced considerably in recent years, due in large part to increases in the power of available computers. Here we use the term "physical modeling" to refer to modeling in which the fundamental equations of mechanics are applied directly to the realistic geometry of a musical instrument. For instruments such as the piano and guitar, this involves solution of the Newton's law equations describing strings, plates, and bars, to describe the body of the instrument, together with the equations of linear acoustics to describe the motion of the air around the instrument and the acoustic field that is produced. The situation is considerably more complicated for wind instruments, for which the equations of linear acoustics must be replaced by the Navier-Stokes (NS) equations. The NS equations are required to describe the complicated fluid motion that takes place in the mouthpiece of wind instruments and the shock waves that can be important in brass instruments.

In recent years, NS-based simulations of wind instruments have been reported by several groups (see, for example, [1, 2, 3, 4, 5, 6, 7]), and the author has reported studies of the recorder in three dimensions [8] that reproduce the behavior of the instrument well. The present paper describes the application of NS-based simulations to a problem encountered in many wind instruments; namely, the flow of air near a tonehole. We study the velocity field near a recorder tonehole, finding significant nonlinear effects at high blowing speeds and study how these effects depend on the length and shape of the tonehole. Our results are in good general agreement with experimental studies carried out with broadly similar (but not identical) geometries. Our results also suggest one reason why undercutting of a tonehole can affect, and presumably improve, the tonal properties of an instrument.

2 Method

Direct numerical simulations of the Navier-Stokes equations were carried out using the method described previously [8]. In that paper the simulations were applied to a three dimensional model of a recorder without toneholes; here we add a single tonehole as shown in Fig. 1. The tonehole was inserted a distance $L_t = 27$ mm from the open end of the recorder whose total length was $L = 105$ mm. The bore of the recorder was square ($d \times d = 10 \times 10$ mm^2). The channel height was $h = 1.0$ mm, the channel length was $L_c = 40$ mm and the channel-labium distance was $W = 4.0$ mm.

Three tonehole geometries were studied, with dimensions given in Table 1. Toneholes 1 and 2 were rectangular in shape, Fig.1(b), and extended the full width d of the channel. Tonehole 3 was similar in shape except that it was undercut at an angle of 45°, Fig. 1(c).

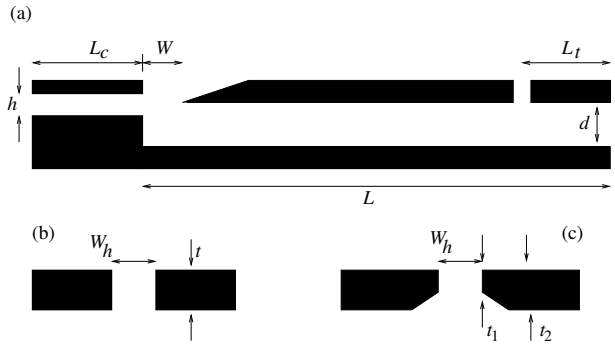

Figure 1: (a) Geometry of the recorder model studied in this work (not to scale). (b) Toneholes 1 and 2 (Table 1) were rectangular with widths W_h and length t. (c) Tonehole 3 was undercut at an angle of 45°.

	tonehole 1	tonehole 2	tonehole 3
	short channel	tall channel	45° undercut
W_h	1.6 mm	1.6 mm	1.6 mm
t	1.6 mm	4.8 mm	—
t_1	—	—	0.8 mm
t_2	—	—	1.6 mm

Table 1: Dimensions of the three toneholes studied in this work. All three were the same distance L_t (see Fig. 1) from the end of the recorder tube.

The simulations were performed as described in [8], using a direct numerical solution of the Navier-Stokes equations employing the MacCormack method [9]. The recorder blowing speed was ramped linearly from zero to a value u_0 in 5 ms, and then held fixed for the rest of the simulation. The sound pressure as a function of time was recorded at various locations inside and outside the recorder, and a steady state oscillation was reached typically between 10 and 20 ms after blowing commenced. After reaching steady state, the density and velocity fields in and around the instrument were recorded for one full period of the oscillation.

3 Results

Figure 2 shows a typical "snapshot" of the density both inside and outside the recorder. Note that this figure, and others below, focus on the region near the recorder; the simulation region is much larger than shown here [8]. These results, and all of the results shown below for the velocity field, were obtained after reaching steady state.

Figure 2 shows calculated results for the air density. Deviations of the density from the background density (i.e., the density in the absence of a sound field) are proportional to the acoustic pressure, so Fig. 2 is essentially also a map

of the acoustic pressure. Here the color indicates the value of the acoustic pressure, with red/brown showing a small value and dark blue indicating a large acoustic pressure. As expected, the sound intensity is much greater inside the tube than outside. The dark blue region in the recorder tube indicates a high sound intensity midway between the labium and the tonehole, which tapers to the background value at both ends. This is simply a standing wave with a wavelength twice the labium-tonehole distance, as expected for the fundamental mode of the recorder with an open tonehole.

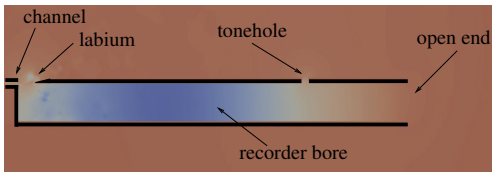

Figure 2: Spatial map of the density showing a standing wave inside recorder tube. The black lines show the borders of the recorder and along the tube they are approximately the thickness of the tube. The recorder was blown from the far left. Results obtained with tonehole 1 and blowing speed $u_0 = 40$ m/s.

Figures 3 and 4 show the velocity field near a short tonehole (tonehole 1 in Table 1) for two values of the blowing speed u_0 at one instant during the oscillation cycle, which had a frequency of approximately 1500 Hz. For the low blowing speed of $u_0 = 20$ m/s (Fig. 3) the velocity near the tonehole and inside the tube is directed mainly along the tube. There are only sight deviations of the velocity from this direction except at the approach to the tonehole and inside the tonehole itself where the flow is upward out of the tonehole; this upward flow continues outside the tonehole. Note that at other times during an oscillation cycle the flow is inward through the tonehole, but within the recorder tube the direction of the velocity is mainly parallel to the recorder tube for this value of the blowing speed.

The behavior with tonehole 1 at the higher blowing speed of $u_0 = 40$ m/s is shown in Fig. 4. The oscillation frequency at this value of the blowing speed is again equal to the fundamental frequency of the recorder; the transition to an oscillation at the second harmonic comes at the somewhat larger blowing speed of about 45 m/s. The form of the velocity field in Fig. 4 is quite different from that found at the lower blowing speed. With this higher value of u_0 there is a pronounced vortex formed inside the recorder and just upstream from the tonehole. Figure 5 shows this vortex at a different time in the oscillation cycle. The vortex is again seen to distort the velocity field over more than half the width of the recorder tube. Even though the flow through the tonehole is now inward, the vortex is quite similar to the one seen in Fig. 4.

Figures 3-5 show the velocity field at particular instants in time, and one could worry that the observation or non-observation of vortices might depend on the precise time at which the velocity field is recorded. We have therefore also analyzed the results of the same simulations by averaging the velocity field over an entire cycle of an oscillation. This should reveal streaming effects [10] as would be expected at high sound amplitudes (e.g., [11]). Average velocity fields for the short tonehole are shown in Fig. 6 (for $u_0 = 20$ m/s) and Fig. 7 ($u_0 = 40$ m/s). These results were obtained in the same simulations as considered in Figs. 3-5.

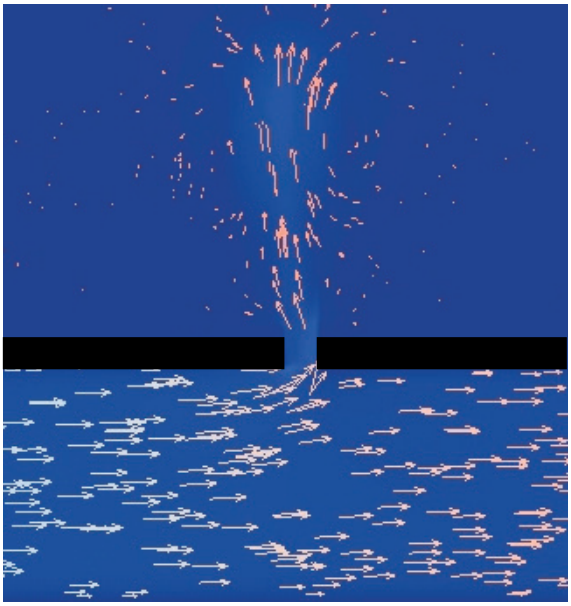

Figure 3: Results for the velocity field near the tonehole obtained with tonehole 1 and a relatively low value of the blowing speed, $u_0 = 20$ m/s. The arrows show the direction of the velocity and their lengths are proportional to its magnitude. This result was obtained at one instant during an oscillation cycle. The black regions are the top wall of the recorder and the open end of the recorder is beyond the right edge of the figure. The bottom edge of the recorder tube is at the bottom edge of this figure.

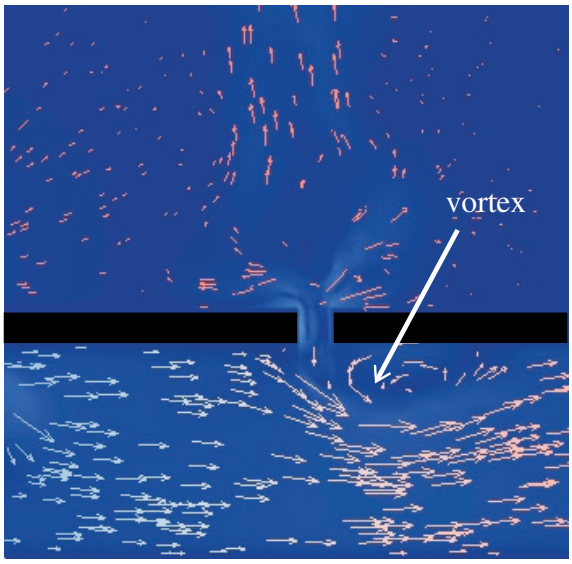

Figure 4: Results for the velocity field obtained with tonehole 1 and a high value of the blowing speed, $u_0 = 40$ m/s. As in Fig. 3, the arrows show the direction of the velocity and their lengths are proportional to its magnitude. Note that the scale factor relating the lengths of these arrows to the magnitude of the velocity are different than in Fig. 3. The black regions are the top wall of the recorder, and the bottom edge of the recorder tube is at the bottom edge of this figure.

Considering first the result for the low blowing speed, Fig. 6, the flow velocity inside the tube is seen to be uniformly to the right over nearly the entire cross-section of the tube. This is not surprising, since the recorder is blown

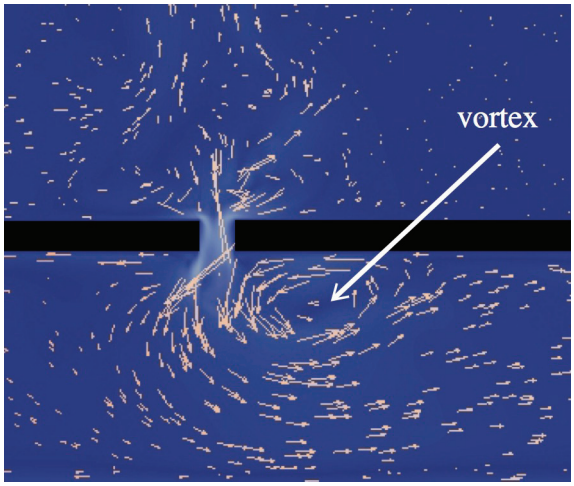

Figure 5: Another view of the the vortex formed near tonehole 1 with $u_0 = 40$ m/s. This result was obtained in the same calculation as in Fig. 4, but at a slightly different time in an oscillation cycle. The black regions are the top wall of the recorder, and the bottom edge of the recorder tube is at the bottom edge of this figure.

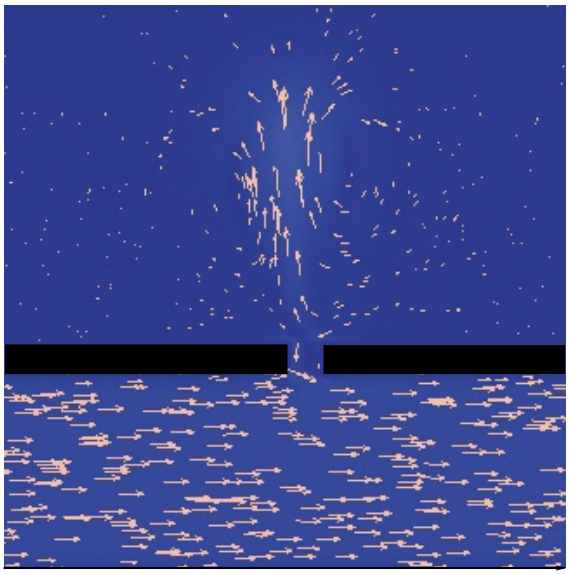

Figure 6: Results for the velocity field averaged over one complete oscillation cycle with tonehole 1 and a low value of the blowing speed, $u_0 = 20$ m/s. The black regions are the top wall of the recorder. The bottom edge of the recorder tube is at the bottom edge of this figure.

through the channel from left to right (Fig. 1), so the net flow averaged over an entire oscillation cycle, must also be from right to left.

At the high blowing speed considered in Fig. 7, a vortex is again found inside the tube and just downstream from the tonehole. The vortex noted earlier for this blowing speed is thus not an artifact of the particular time at which the velocity field is recorded and it does not disappear on averaging, a signature of acoustic streaming. Just outside the tonehole, there appears to be a slight tendency for flow to the left, which is opposite to the direction of net flow inside the tube. This counterflow is more pronounced at the higher blowing speed (Fig. 7) but there is also a small effect that is of marginal size at the lower blowing speed (Fig. 6). We believe that it is significant, but more study

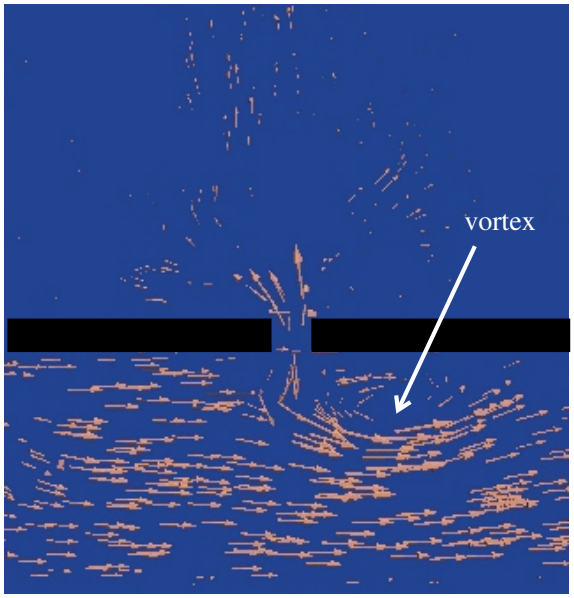

Figure 7: Results for the velocity field averaged over one complete oscillation cycle with tonehole 1 and a high value of the blowing speed, $u_0 = 40$ m/s. The black regions are the top wall of the recorder. The bottom edge of the recorder tube is at the bottom edge of this figure.

will be required to confirm this, for the following reason. In our simulation the recorder is in a closed region, so there must be some return flow from the open end of the recorder (on the far right, not shown in Fig. 7) back to the entrance to the recorder on the far left. It is worth noting that the counterflow effect outside the tonehole in Fig. 7 is similar to that observed experimentally in a related geometry [12].

All of the results in Figs. 3-7 were obtained with the short tonehole (tonehole 1). We studied several toneholes with different lengths; these were rectangular in cross-section and with the same width in the direction perpendicular to the plane in Fig. 1 but with recorder walls of different thickness. (The cross-section of the recorder tube was the same in all cases.) Results for a tonehole that is taller than tonehole 1, the tonehole considered in Figs. 3-7, are shown in Fig. 8. This tonehole is denoted tonehole 2 in Table 1 and is three times longer than tonehole 1. Figure 8 shows results with the high blowing speed $u_0 = 40$ m/s averaged over one cycle of the oscillation. A vortex is now barely visible inside the tube and upstream from the tonehole; this vortex is much smaller in size than found with the short tonehole.

The toneholes in many instruments are undercut, with their open area being smaller at the exit end of the tonehole, as sketched in Fig. 1(c). Tonehole 3 in Table 1 was undercut in this way, and results for that tonehole are shown in Fig. 9. Here again we consider the high blowing speed $u_0 = 40$ m/s and the velocity field is averaged over one cycle of the oscillation. There is now no vortex inside the tube. The shape of the tonehole thus has a very pronounced effect on the behavior.

4 Discussion

There have been a number of theoretical studies of toneholes, both analytical and numerical; for a partial list see [13, 14, 15, 16, 17, 18, 19, 20]. These theoretical

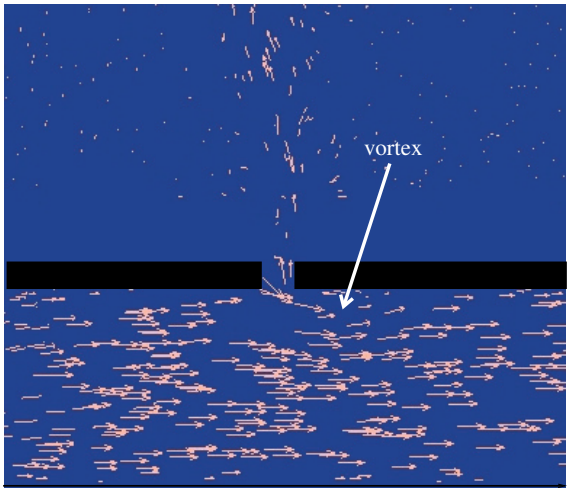

Figure 8: Results for the velocity field averaged over one complete oscillation cycle with tonehole 2 and a high value of the blowing speed, u_0 = 40 m/s. The black regions are the top wall of the recorder. The bottom edge of the recorder tube is at the bottom edge of this figure.

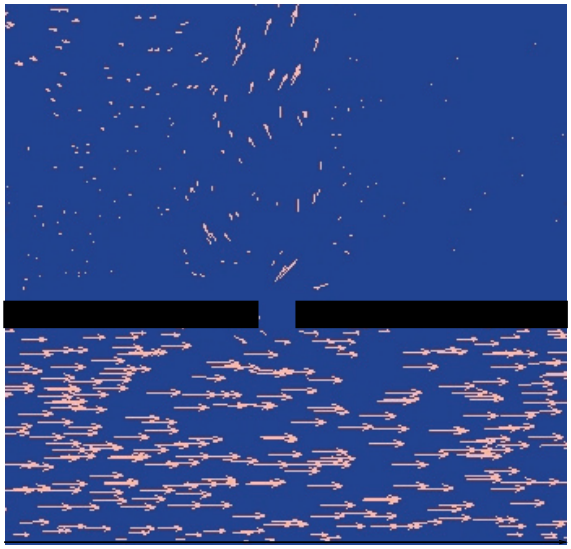

Figure 9: Results for the velocity field averaged over one complete oscillation cycle with tonehole 3 and a high value of the blowing speed, u_0 = 40 m/s. This tonehole was undercut as described in Table 1. The black regions are the top wall of the recorder. The bottom edge of the recorder tube is at the bottom edge of this figure.

studies have thoroughly explored the linear behavior and while the importance of nonlinear behavior has been noted by several workers, much remains to be understood in the nonlinear regime. Experimental studies of the velocity fields near toneholes have been carried out using particle image velocimetry, and our results are broadly consistent with those results. For example, the presence of an upstream vortex inside the instrument tube has been observed in several studies [12, 21, 22]. Consistent with our results, these vortices are only observed at high intensities, confirming that they are a nonlinear effect. In addition, undercutting of the tonehole has been found to suppress this vortex [22]. Much more work remains to compare our computational results with the experiments. In particular, the experiments in [12, 21, 22] were all carried out using tubes in which the sound field was produced by a speaker so that the frequency could be continuously varied. This contrasts with our studies in which a full instrument was modeled and hence the frequency was determined by the resonance conditions of the instrument.

5 Conclusion

We have presented detailed results for the velocity field near a tonehole in a three dimensional recorder. The results are broadly consistent with experimental studies, as at high sound levels we observe a vortex inside the recorder tube and downstream from the tonehole. This vortex is largest for short toneholes and is suppressed by undercutting of the tonehole. While our work has focused on the behavior of a single tonehole, it is interesting to speculate on the case of multiple toneholes. Some years ago Keefe [15] found that the addition of two closely spaced toneholes to the end of a model clarinet made it extremely difficult to produce a musical tone with the instrument. Given the size of the vortex we have found in some cases, it is intriguing to speculate that a nonlinear interaction between toneholes, mediated by such vortices, may play a role in such cases. This could also explain why the undercutting of toneholes, which acts to suppress these vortices, is common in many instruments. These speculations will be object of future study. Also left for the future is to study the effect of tonehole geometry on the tonal properties.

Acknowledgments

The author thanks the Rosen Center for Advanced Computing at Purdue University for access to the computational resources essential for this work.

References

[1] A. Skordos and G. J. Sussman, “Comparison between subsonic flow simulation and physical measurements of flue pipes,” in Proceedings of the International Symposium on Musical Acoustics, Dourdan, France (1995), pp. 1-6.

[2] H. Kühnelt, “Simulating the mechanism of sound generation in flutes and flue pipes with the lattice-Boltzmann-method,” in Proceedings of the International Symposium on Musical Acoustics, Nara, Japan (2004), pp. 251-254.

[3] H. Kühnelt, “Vortex sound in recorder- and flute-like instruments: Numerical simulation and analysis,” in Proceedings of the International Symposium on Musical Acoustics, Barcelona, Spain (2007), pp. 1-8.

[4] R. D. Silva, H. Küuhnelt, and G. Scavone, “A brief survey of the lattice- Boltzmann method,” in Proceedings of the International Congress on Acoustics, Madrid, Spain (2007), pp. 1-6.

[5] Obikane and K. Kuwahara, “Direct simulation for acoustic near fields using the compressible Navier-Stokes equation,” Comput. Fluid Dyn. J. 2008/2009, 85-91 (2009).

[6] Miyamoto, Y. Ito, K. Takahashi, T. Takami, T. Kobayashi, A. Nishida, and M. Aoyagi, "Applicability of compressible LES to reproduction of sound vibration of an air-reed instrument," in Proceedings of the International Symposium on Musical Acoustics, Sydney and Katoomba, Australia (2010).

[7] N. Giordano, "Direct numerical simulation of a recorder," *J. Acoust. Soc. Amer.* **133**, 1111-1118 (2013).

[8] N. Giordano, "Simulation studies of a recorder in three dimensions," *J. Acoust. Soc. Amer.* **135**, 906-916 (2014).

[9] R. W. MacCormack, "The effect of viscosity in hypervelocity impact cratering, *AIAA* Pap.**68**-354, 1-7 (1969).

[10] J. Lighthill, "Acoustic streaming." *J. Sound and Vibration* **61**, 391-418 (1978).

[11] J. P. Sharpe, C. A. Greated, C. Gray, and D. M. Campbell, "The measurement of acoustic streaming using particle image velocimetry," *Acustica* **68**, 168-172 (1989).

[12] D. J. Skulina, R. MacDonald, and D. M. Campbell, "PIV applied to the measurement of the acoustic particle velocity at the side hole of a duct," *Forum Acusticum Budapest*, p. 507-512 (2005).

[13] D. H. Keefe, "Theory of the single woodwind tone hole," *J. Acoust. Soc. Am.* **72**, 676-687 (1982).

[14] D. H. Keefe, "Experiments on the single woodwind tone hole," *J. Acoust. Soc. Am.* **72**, 688-699 (1982).

[15] D. H. Keefe, "Acoustic streaming, dimensional analysis of nonlinearities, and tone hole mutual interactions in woodwinds," *J. Acoust. Soc. Am.* **73**, 1804-1820 (1983).

[16] C. J. Nederveen, "Corrections for woodwind tone-hole calculations," *Acta Acustica united with Acustica* **88**, 957-966 (1998).

[17] A. Richter, unpublished (2007). Referenced and with some results shown in [22].

[18] A. Lefebvre and G. P. Scavone, "Characterization of woodwind instrument toneholes with the finite element method," *J. Acoust. Soc. Am.* **131**, 3153-3163 (2012).

[19] A. Lefebvre, G. P. Scavone, and J. Kergomard, "External tonehole interactions in woodwind instruments," *Acta Acustica united with Acustica* **88**, 975-985 (2013).

[20] T. Iwasaki, K. Takahashi, T. Takami, A. Nishida, and M. Aoyagi, "Numerical study of the function of tone holes of a recorder like instrument from the viewpoint of the aerodynamic sound theory," *Proc. Meetings on Acoustics* **19**, 035024 (2013).

[21] D. Rockliff, "Application of particle image velocimetry to the measurement of non-linear effects generated by high-intensity acoustic fields," Ph. D. thesis, University of Edinburgh (2002).

[22] R. MacDonald, "A study of the undercutting of woodwind toneholes using particle image velocimetry," Ph. D. thesis, University of Edinburgh (2009).